Contents list available at IJRED website

International Journal of Renewable Energy Development

Journal homepage: https://ijred.undip.ac.id

Research Article

The Design and Analysis of a Novel Vertical Axis Small Water Turbine Generator for Installation in Drainage Lines

Werayoot Lahamornchaiyakul* and Nat Kasayapanand

Division of Energy Technology, School of Energy, Environment and Materials, King Mongkut's University of Technology Thonburi, 126 Pracha-Uthit Road, Bang Mod, Thungkhru, Bangkok, 10140, Thailand

Abstract. The objective of this study was to determine the mechanical power efficiency of a novel vertical-axis small water turbine generator for installation in drainage lines. A 3D model was created to evaluate the performance of each design. The system was designed, analysed, and calculated for the most suitable geometries of the water inlet, drainage lines, main structure, and water turbine wheels using computational fluid dynamics software. The diameter of the water turbine wheel in the numerical model was 48 mm. The control volume technique was used in the numerical simulation method, and the k-epsilon turbulence model was employed to find the computational results. For the Computational Fluid Dynamics (CFD), the appropriate mash element for each model section was generated for numerical simulation, which showed that the torque from the water turbine modelling varied depending on the time domains and was related to speed relative to the developed force. The maximum torque and maximum power that a vertical-axis small water turbine for installation in a drainage line could generate at a maximum flow rate of 0.0030 m^3/s were 0.55 N.m and 26.84 watts, respectively. Similarly, calculations with mathematical equations, found that the maximum mechanical power value after calculating the rate of loss within the pipe system was 12.95 watts. The forces generated by the speed and pressure of the fluid can then be applied to the structure of the water turbine wheel. The vertical-axis small water turbine for installation in a drainage line was analysed under its self-weight by applying a gravitational acceleration of 9.81 m/s^2 in Solidworks Simulation software version 2022. The numerical simulations that resulted from this research could be used to further develop prototypes for small water turbines generating commercial electricity.

Keywords: computational fluid dynamics, finite element analysis, 3d design, vertical axis water turbine, drainage line

Received: 18th August 2022; Revised: 22nd Dec 2022; Accepted: 4th Jan 2023; Available online: 7th Jan 2023

1. Introduction

Energy generated from water can be considered clean energy. Water is a natural resource with a very high potential for generating electricity from its movement and has the added benefit of not polluting the environment (Sritram *et al.,* 2017; Chen *et al.,* 2021). At present, hydro power is becoming more popular as a renewable form of energy because the cost of production is low compared to other energy sources (Olatunji *et al.,* 2018; Tiaple *et al.*, 2008). Usually, the production of electricity from water requires the construction of large dams and relies on the difference in water level (head) as the main variable in energy generation. A significant level of difference is required to create flow rates with high speeds. The flow speeds of water in streams and rivers can also be used to design water turbines that generate electricity. Saving water and energy continues to be one of the world's top priorities and this is likely to remain the case in the near future (ESHA, 2010). Over recent years, there has been a great deal of research supporting the idea of creating new forms of electricity that rely on the water flow in closed pipelines to generate electrical energy for various equipment such as data recorders and water leak sensors (Chen *et al.,* 2013). A water turbine is a device used to extract energy generated from the water flow in a pipeline. Installing water turbines in pipeline systems has been studied and fluctuations revealed in pressure systems of different origins and destinations (Thomas *et al.,* 2019). Therefore, technical information such as flow rate, flow pressure, pipe sizing, and pipe fittings is very useful in the design of highly efficiency water turbines for installation in pipelines. This is because the pressure loss in the flow rate must be considered (Muhammad *et al.,* 2021). The Mueang Phitsanulok District in Thailand is known to have a large network of water supply pipes. This is true for several large urban areas and urban communities in the provinces, but they are often not used effectively to generate energy in comparison to developed countries. In addition, the sewer pipes from buildings and houses in Phitsanulok Province are still underrepresented in terms of generating energy from sewage. The sewer pipes from buildings and houses can also be modified for power generation. In recent times, feasibility studies have been undertaken on power generation using a pico-hydraulic turbine from sewage flowing in pipes (Uchiyama *et al.,* 2016; Ghada *et al.,* 2022). The sewage from sewer pipes includes rainwater and water, as well as waste released by humans and manufacturing operations into the sewers (Cabra, 2014; Tahir *et al.,* 2020). Sewer systems also contain human waste from homes, workstations, and industrial sectors. Besides, a report on the design of water turbines for extracting energy from sewerage reveals that the runner features a hollow drum around the main axis to allow waste material to pass

* Corresponding author:
Email: werayootrmutl@gmail.com (W.Lahamornchaiyakul)

https://doi.org/10.14710/ijred.2023.48388
ISSN: 2252-4940/© 2023.The Author(s). Published by CBIORE

through. Wastewater comprises domestic hair and vegetable waste, as well as culinary garbage and human waste. To properly create electricity from sewage, turbines must remain free from clogging caused by waste (Sinagra *et al.,* 2014; Tahir *et al.,* 2020). According to the principles and significance of pipeline energy production, resulting activities include researching and developing small water turbines for use in drainage systems to generate electrical energy. Therefore, the development of different types of water turbines that operate effectively according to the type of work is currently very important, because water turbines capable of generating electricity as a kind of fluid machinery are important for hydroelectric power generation.

Small water turbines for installation in pipelines are classified into vertical and horizontal axis according to their rotation. Vertical-axis turbines have the advantage of operating independently of incident flow direction and achieving higher efficiency at lower speeds. Based on the driving force, vertical-axis turbines are either drag- or lift-based. Water turbines have been studied, investigated, and introduced through numerous research projects. (*e.g.,* Ghada *et al.,* 2022; Chen *et al.*, 2013; Hasanzadeh *et al.,* 2021; Jiyun et al., 2018; Ma *et al.,* 2018; and Samora *et al.,* 2016). However, these studies revealed that the power output of a vertical-axis small water turbine for installation in pipelines is rather low, with considerable accompanying pressure losses. This can have a considerable impact on the overall picture of price and performance in generating electricity. Therefore, the design of working systems to predict behavior prior to actual construction is critical in practice (Posew et al., 2016). At present, a large number of designs and measurement tools are available for water turbines that generate electricity, such as various test equipment and the rotational meter, torque measurement and instruments for measuring power, as well as vibration meters. The design, building and testing of a real prototype require significant investment making it unpopular among modern researchers. Consequently, a new approach involves the introduction of technology to computational fluid dynamics to help design the flow field. In addition, finite element analysis is used to simulate the structural strength of the water turbines, etc. (Yeo *et al.,* 2019). The OpenFOAM program has been used to help simulate vertical axis turbines installed in piping systems to monitor performance (Temidayo *et al.,* 2018). A study on fluid dynamic simulation has been conducted using the Autodesk Flow Simulation program to assess the hydroelectric feasibility of turbines in pipes for water line optimization based on the time series of water supply rates (Jiyun, *et al.,* 2017). Other, studies have been conducted on optimizing the shape and geometric parameters of blocks for speeding up numerical simulation methods to improve the efficiency of water turbines using the ANSYS FLUENT 14.5 program (Culafic, *et al.,* 2020). Besides, studies on the distribution of stress values occurring in water pipe structures have been conducted with the stress analysis module in the Autodesk Inventor Professional version 2016 (Autodesk Inventor, 2015). The results from the previously mentioned research demonstrate the importance of designing and simulating the numerical effects of water turbines in generating electricity for installation in pipeline systems. Therefore, it is necessary to recognize the significance of unused energy patterns within the drainage lines of buildings or houses and researchers are becoming increasingly interested in them. Thus, the design of low-cost water turbine blade wheels and the proper installation of a newly designed turbine kit in Thailand's drainage line systems require the use of computational fluid dynamics and finite element analysis techniques.

(a)

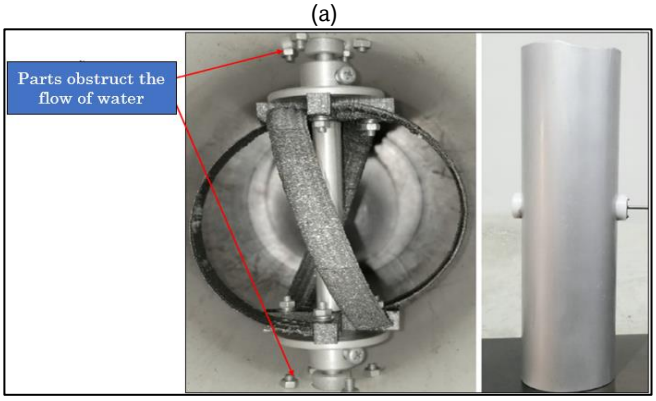

(b)

Fig. 1 The problems in this research are: (a) a specially designed water pipeline layout (Marco, 2015); (b) parts that obstruct the flow of water turbines in pipes (Muhammad *et al.,* 2021)

According to previous research on water turbines installed within a piping system, the cost of design and production is very high since pipe sizes need to be designed with specific cross-sectional areas. Moreover, the installation still requires equipment inside the pipe, such as nuts and screws, directly affecting the loss in flow rate, as shown in Fig. 1. Also, considering that a water flow rate enters one end of a piping system and leaves the other, a pressure drop or loss is inevitable. The friction caused by fluids rubbing against piping components and the interior walls of a piping system results in a pressure drop.

Based on the issues depicted in Fig. 1, a new water turbine that could simplify installation and be attached to existing PVC water pipelines without changing the pipe size is proposed in this study. The installation process is determined by the shape of the sewer pipe with its cylinder structure and circular cross-section, and the position of the water turbine is installed between the elbows at 45 degrees. The redesigned water turbine is presented in Fig. 2. Fig. 2 shows the design of a two-wheel vertical-axis water turbine installed inside a parallel drainage line to reduce space and loss caused by the obstruction of water flow. The consideration of data was prioritized in the design since it determines the shape of the DC 12V Model GOSO F50-12V. A small generator, purchased from Shenzhen Global Technology, was also employed, (readily available on the market). Part 2: The data and installation location were then considered to enable the model to be properly assembled into a drainage line.

The objective of this study is to design a new water turbine which can reduces the installation process, be attached to a PVC water pipeline readily available on the market without adapting the pipe size, and reduce the effects of flow loss caused by nuts and screws. Moreover, it can be applied to the drainage lines installed in selected areas of Phitsanulok Province, Thailand

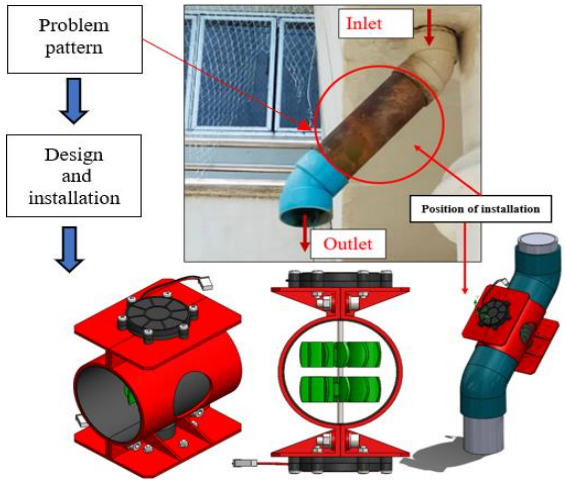

Fig. 2 Position of the installation and design for a small vertical-axis water turbine

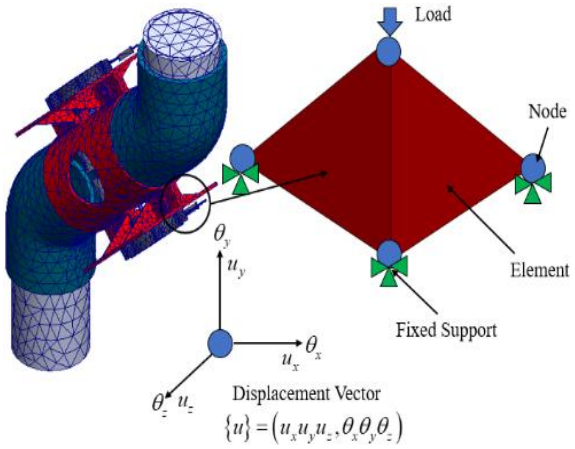

Fig.3 Details of the FEA Mesh Element

2. Numerical Simulation Model

2.1 CFD Model

The incompressible flow pattern through turbomachinery is described using the continuum and momentum theory, known as the Navier-Stokes equation. The CFD model of a novel vertical-axis small water turbine for installation in drainage lines in this research can be seen in Navier-Stokes equations, which are expressed by Equations 1–4 (Mosbahi *et al.,* 2019; McLean, 2012; Muhammad *et al.,* 2021; Anas *et al.,* 2022; Wisatesajja *et al.,* 2021).

$$\frac{\partial \rho}{\partial t} + \frac{\partial (\rho u_i)}{\partial x_i} = 0 \quad (1)$$

$$\frac{\partial (\rho u_i)}{\partial t} + \frac{\partial}{\partial x_j}(\rho u_i u_i) + \frac{\partial P}{\partial x_i} = \frac{\partial}{\partial x_i}(\tau_{ij} + \tau_{ij}^R) + S_i \quad (2)$$

$$\frac{\partial \rho H}{\partial t} + \frac{\partial \rho u_i H}{\partial x_i} = \frac{\partial}{\partial x_i}(u_j(\tau_{ij} + \tau_{ij}^R) + q_i) + \frac{\partial p}{\partial t} - \tau_{ij}^R \frac{\partial u_i}{\partial x_j} + \rho\varepsilon + S_i u_i + Q_H \quad (3)$$

$$H = h + \frac{u^2}{2} \quad (4)$$

Solidworks Flow Simulation software employs transport equations for the turbulence kinetic energy by using the model (Patel *et al*., 2016; Nasir, 2013), which is shown in equations (5) -(8) (Sobachkin *et al.,* 2013; Hosain *et al.,* 2020).

$$\frac{\partial \rho k}{\partial t} + \frac{\partial \rho k u_i}{\partial x_i} = \frac{\partial}{\partial x_i}\left(\left(\mu + \frac{\mu_t}{\sigma_k}\right)\frac{\partial k}{\partial x_i}\right) + \tau_{ij}^R \frac{\partial u_i}{\partial x_j} - \rho\varepsilon + \mu_t P_B \quad (5)$$

$$\frac{\partial \rho \varepsilon}{\partial t} + \frac{\partial \rho \varepsilon u_i}{\partial x_i} = \frac{\partial}{\partial x_i}\left(\left(\mu + \frac{\mu_t}{\sigma_\varepsilon}\right)\frac{\partial \varepsilon}{\partial x_i}\right) + C_{\varepsilon 1}\frac{\varepsilon}{k}\left(f_1 \tau_{ij}^R \frac{\partial u}{\partial x_j} + C_B \mu_t P_B\right) - f_2 C_{s1}\frac{\rho\varepsilon^2}{k} \quad (6)$$

$$\tau_{ij} = \mu S_{ij}, \tau_{ij}^R = \mu_t S_{ij} - \frac{2}{3}\rho k \delta_{ij}, S_{ij} = \frac{\partial u_i}{\partial x_j} + \frac{\partial u_j}{\partial x_i} - \frac{2}{3}\delta_{ij}\frac{\partial u_k}{\partial x_k} \quad (7)$$

$$P_B = -\frac{g_i}{\sigma_B}\frac{1}{\rho}\frac{\partial \rho}{\partial x_i} \quad (8)$$

where $C_\mu = 0.09, C_{\varepsilon 1} = 1.44, C_{\varepsilon 2} = 1.92, \sigma_k = 1,\ \sigma_\varepsilon = 1.3, \sigma_B = 0.9, C_B = 1\ if\ P_B > 0, C_B = 0$

If considering $P_B < 0$, the turbulence viscosity is determined from $\mu_t = \frac{C_\mu \rho k^2}{\varepsilon}$

Note: In a simple flow experiment, water and air are used to calculate and determine the values of these constants.

2.2 FEA Model

In this case, the governing equation for the linear static finite element analysis is determined by equation (9) (Lahamornchaiyakul, 2021; Vaishaly *et al.,* 2015).

$$[K]\{q\} = \{F\} \quad (9)$$

where $[K]$is Structural stiffness; $\{q\}$ Nodal displacement and $\{F\}$ Load matrix

The finite element model consists of a node and an element. In this case, it is found that the degree of freedom has a maximum of 6 independent variables when considering only one node. The finite element model in this case is shown in Fig. 3.

3. Water Turbine Design

In this case, the designing procedure consists of finding the parameters associated with the vertical axis water turbine generator for installation in drainage lines. They are as follows:

3.1 Net Head (H_n)

In this study, the net head is the differences between the gross head and the equivalent losses (Patel *et al.,* 2016). The net head in this study is shown in Fig. 4.

$$H_N = H_g - H_l \quad (10)$$

Where $H_l$is the head equivalent for the different losses in the drainage line, H_g is the gross head at the tank of the water turbine (Patel et al., 2016).

In this study, the gross head of the small vertical axis water turbine for installation in a drainage line was determined in this study at 0.625 m. Consideration must be given to rainfall uncertainty when a small water turbine is installed in a drainage line. Moreover, it is difficult to ascertain from previous rainfall data on Phitsanulok Province how much water can be obtained from rain. Moreover, the average rainfall has the potential to drain into sewage systems to generate energy with a small water turbine. Phitsanulok Province is located at latitude 16.78 north, longitudinal 100.20 east, and about 44 m (144 feet) above sea level. The average rainfall throughout the year is about 1400.8 mm. (Sukha *et al.,* 2019). The majority of the area around Phitsanulok Province consists of structures with decks or buildings that have been partially transformed into smaller decks for water retention, as shown in Figs. 2 and 4.

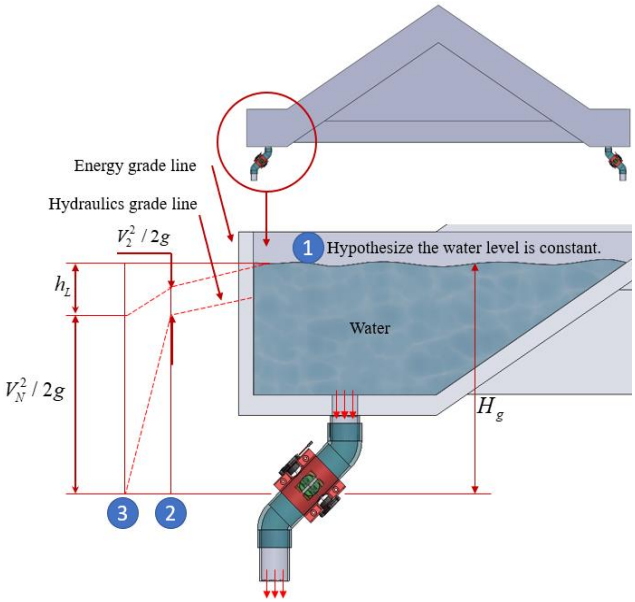

Fig. 4 Illustration of the net head

When it rains, the area is well-supported for water collection. Furthermore, the rainfall in the deck area is drained by sewer pipes in the next step. A diagram of the area receiving rainwater before being drained from the roof of a building is presented in Fig. 4. It can be hypothesized that the water level is constant and this information can be used as a starting point for water turbine design.

*3.2 Water Flow Rate (**Q**)*

In this study, the water flow rate is calculated by measuring the velocity of water and the cross-section area of the pipeline for water turbine installation, as give in equation (11).

$$Q = Av \ (m^3/s) \tag{11}$$

The water flow rate for the water turbine design in this research was selected as Q = 0.0010, 0.0015, 0.0020, 0.0025, and 0.0030 m^3/s, respectively.

*3.3 Water Turbine Power (**P**)*

It is the power output that is produced by the vertical axis small water turbine generator for installation in the pipeline. The water turbine power can be determined as shown in equations (12).

$$P = \rho g Q H_n \tag{12}$$

3.4 Calculation of mechanical power under the rate of system loss

This section presents, the harvested power of the vertical-axis small water turbine for installation in a drainage line. Rate loss due to rotation speed, arc of the blade, and length of the pipe can be determined by computational fluid dynamics (CFD), as shown in Table 1. The power output can be calculated according to the formula proposed by (El-Sayed *et al.,* 2019).

Based on the insights discussed above, approximately 80% efficiency is applied to the novel vertical-axis small water turbine generator for installation in a pipeline in this research.

$$P = \eta \times \Delta p \times Q \tag{13}$$

Data:
1. Efficiency (η) 80% (0.80).
2. Loss of pressure head (h_L) = 0.55 m.
3. Pipe diameter (D_p) = 50.8 mm. (2 in)
4. Wheel turbine diameter (D_o) = 48 mm.
5. Velocity (V) = 1.481 m/s.

3.5 Turbine Speed (N)

Turbine speed can be calculated from equations (14) and (15) (Ebhota *et al.,* 2015; Abdulah *et al.,* 2022).

$$N = \frac{\omega \times 60}{2\pi} \tag{14}$$

$$\omega = \frac{V}{R} \ (rad/s) \tag{15}$$

where N is the rotation speed (RPM), and ω is the omega velocity, while V is the water speed and R is the radius of the wheel turbine.

For calculating the speed of the rotation of a water turbine, a flow rate of 0.003 m^3/s was determined to calculate the water speed, which was found to be equal to 1.481 m/s. According to the design in this research, a water pipe with a diameter of 50.8 mm was needed, so a water turbine wheel diameter of 48 mm was established.

3.6 Design of blade spacing (t_B)

The tangential blade spacing can be determined from equation (16) (Patel *et al.,* 2016, 2016; Nasir, 2013).

$$t_B = 0.174 \times D_o \ (mm) \tag{16}$$

*3.7 Number of runner blades (**n**)*

In this study, the equation (17) can be written as follows (Patel *et al.*, 2016; Nasir, 2013).

$$n = \frac{\pi \times D_o}{t_B} \tag{17}$$

3.8 Blade radius curvature (r_B)

In this research, the blade radius curvature equation can be written as follows (Patel *et al.*, 2016; Nasir, 2013).

$$r_B = 0.163 \times D_o \tag{18}$$

3.9 Design of the shaft diameter (D_S)

This research involves the optimum design of the shaft diameter for vertical axis small water turbines. It is designed to carry the load of the maximum water force exerted on the water turbine shaft structure. Equation (19) can be used to calculate the shaft diameter.

$$D_S = 0.22 \times D_o \tag{19}$$

Calculation and finding the right proportion for the set of water turbine wheels were done in this research by using the equation system relationship at (13)– (19); the results are shown in Fig. 5.

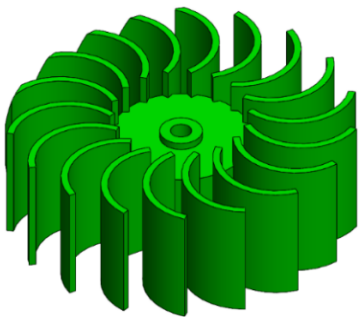

Fig. 5 The number of runner blades in the 3D design

*3.10 Time step calculation using blade passage (**T**)*

The time step size for Computational Fluid Dynamics in this research, can be determined using equation (20) (Oladosu *et al.,* 2018; Autodesk Simulation CFD, 2015).

$$T = D_o/(N \times 6) \quad (20)$$

4. Numerical Simulation Setting

4.1 CFD Simulation Setting

Based on Fig. 1, the gathered information can be used to design a 3D shape using the Solidworks program version 2014, as shown in Fig. 2. According to Fig. 2, the diameter of the water turbine wheel in the numerical model measured 48 mm. The CFD simulation was performed using the Solidworks Flow Simulation. The simulation was carried out in time step of 0.0135 s. This simulation ran for 10 s. The volume flow rate was imposed at the inlet, and the environmental pressure at the outlet boundaries was equal to 101325 Pa. Wheel rotation was predicted using the rotating region module, set to 197, 295, 393, 492, and 590 RPM at volume flow rates of 0.0010, 0.0015, 0.0020, 0.0025, and 0.0030 m^3/s, respectively. The mesh elements in the dependency tests were considered using a standard $k-\varepsilon$ turbulence model. The boundary condition setting in this research is shown in Fig. 6.

4.2 Computational Domain Mashing

Mesh elements can be created in this study using the Solidworks Flow Simulation Program. The entire computational domain was subdivided into about 900,000 quadrilateral mesh elements. The CFD meshing section of Solidworks Flow Simulation was performed to convert the continuous domain to a discrete section. Meshing validation was carried out from the third level mesh to the best mesh (Prasetyo *et al.,* 2018).

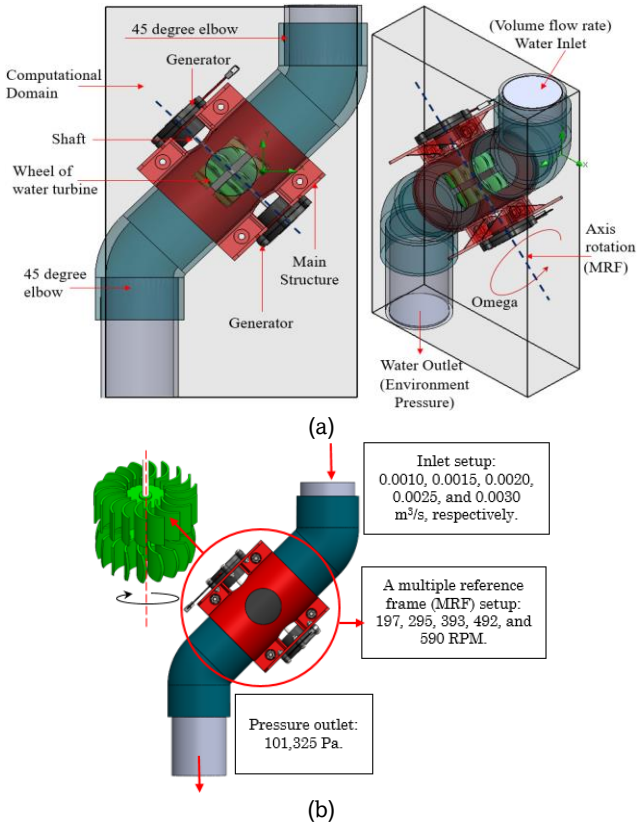

Fig. 6 CFD simulation setting of (a) computational domain and (b) boundary conditions

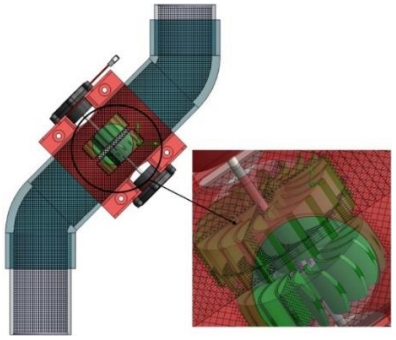

Fig. 7 Illustration of CFD Mesh Structure

The mesh elements of the various sections are illustrated in Fig. 7. According to Fig.7 shows that the meshing of each part is not the same as the element size. The water turbine wheel element size should be the most detailed due to the complexity of the curvature of the water turbine wheel surface.

The residual value of all variables is less than 0.0001. If the calculation meets such conditions, the numerical calculations are considered to approach the answers according to the preliminary requirements, while studying the area where the moving reference frame (MRF) is defined along with the stationary work piece defined as a stationary-type mesh element, which is called a multiple reference frame (MRF).

The goal of setting boundary conditions in CFD is to confine the discrete form of the equation so that it may be solved in a specific framework while also describing the flow parameters of the computational domain.

4.3 Assumptions for CFD Simulation

The CFD results of the vertical axis small water turbine for installation in drainage lines are presented in this section. The analysis and simulation were carried out using commercial software, namely of Solidworks Flow Simulation.

1) The following assumptions were incorporated into the CFD simulation:
   - -The water level is constant.
   - -Analysis type is internal flow.
   - -Rotation type is the local region (sliding).
   - -Gravity is -Y direction equal to-9.81 m/s^2.

2) CFD analysis solution parameters
   - -The periodic is equal to 0.0135 seconds.
   - -The cores and memory usage are 8 cores.

5. Results and Discussion

In this paper, the results of the CFD simulation are presented first, and then the FEA results will be present and discussed.

5.1 CFD Simulation Results

The results of the mesh element test concerning the accuracy of the rotational speed and power output of the water turbine wheels are shown in Fig. 8. The graph shows the relationship between the number of mesh elements, the rotation speed and the power output of the vertical-axis small water turbine over a range of 100,000 to 900,000 elements. As observed, the slope becomes constant when the number of model elements reaches 700,000. Thus, 900,000 elements were used in the CFD simulation.

Fig. 8 graphically depicts increasing the number of mesh elements affects the suitability and accuracy of the analysis results for water turbines in this study. The graph of the power

output variables derived from numerical simulations in Fig. 8 does not show the calculated loss rate of the water turbine system. Due to CFD, the loss rate in the working system of the water turbine cannot be accounted for, and when considering the actual operation, the electrical power variable value is reduced due to the loss rate in the flow system. Fig. 9 shows a flow field of the water speed through a set of water turbine wheels, during the rotation of the water turbine wheels. As shown by positions 1 and 2 in Fig. 9, the eddying locations of the water affect the pressure loss within the piping system. It can be observed that the average velocity remains constant along the pipe except for some deviation immediately around the water turbine rotor in positions 1 and 2. The image depicts the CFD velocity contour results obtained by using a water turbine wheel and flow rates ranging from 0.0010 to 0.0030 m3/s, which had an effect on the water turbine wheel. This resulted in observable weak flow regions and clearly separated turbulent flow layers.

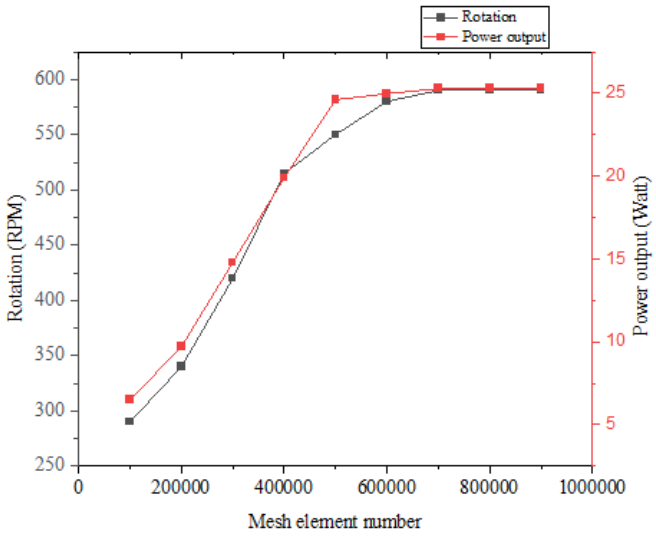

Fig. 8 Graph of mesh elements test results at Q = 0.003 m^3/s

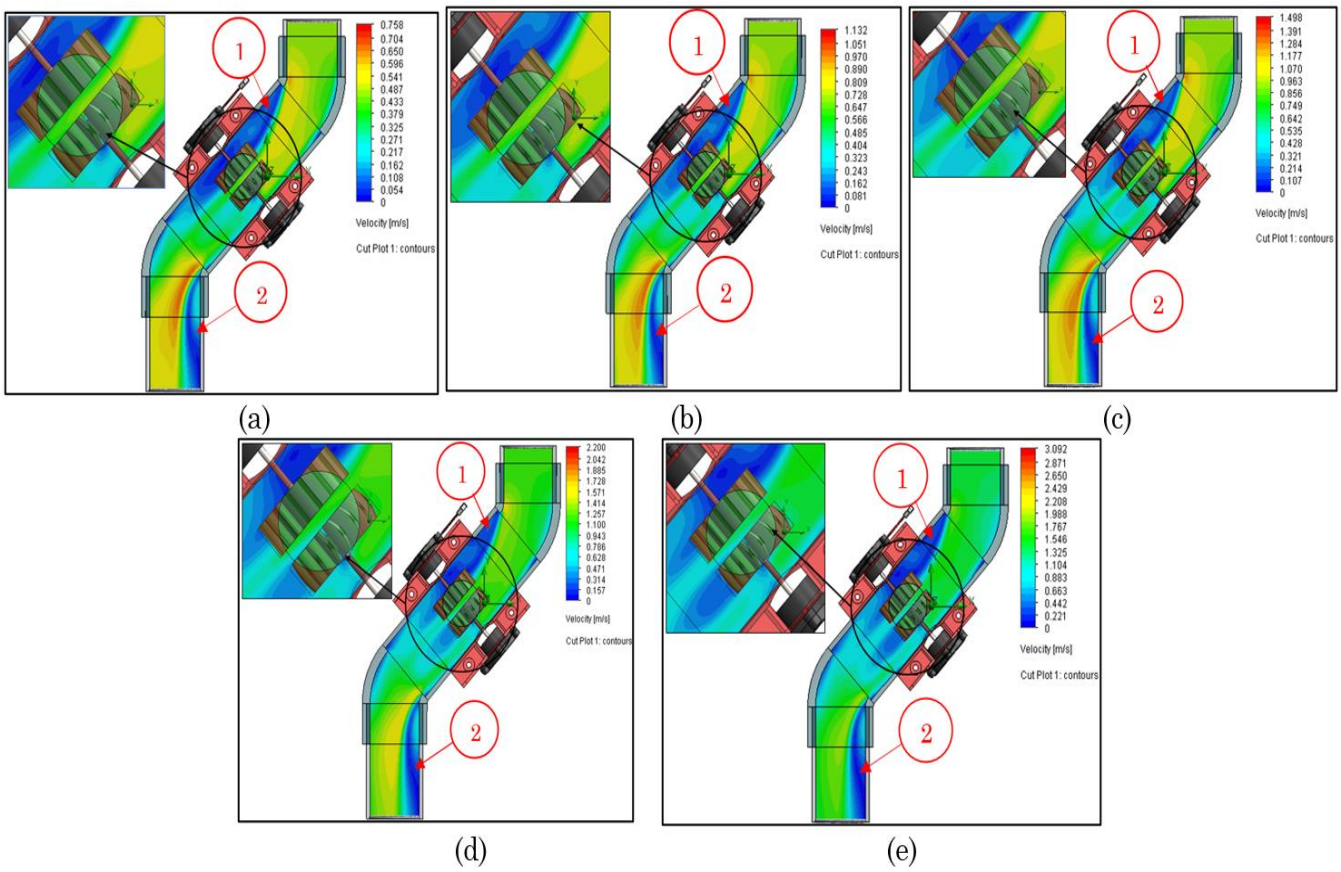

Fig. 9 Water-velocity contour of (a) Q = 0.001 m^3/s, (b) Q = 0.0015 m^3/s, (c) Q = 0.0020 m^3/s, (d) Q = 0.0025 m^3/s, and (e) Q = 0.0030 m^3/s

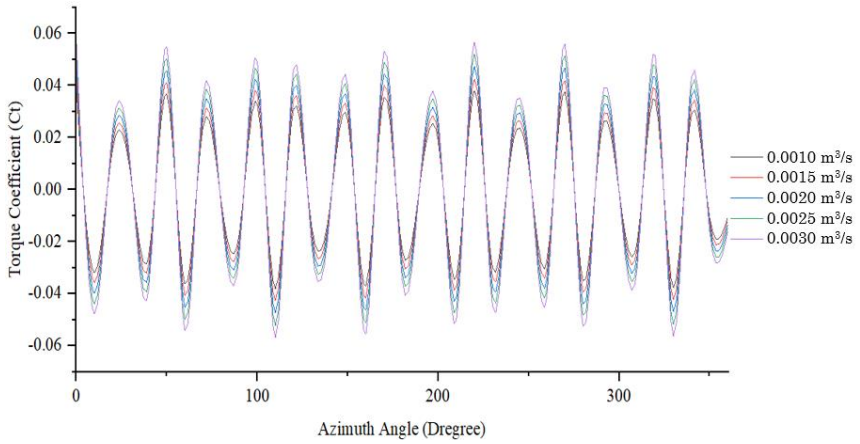

Fig. 10 The dynamic torque coefficient of different flow rates

Since flow characteristics affect turbine performance, this study investigates the flow velocity vectors around the water turbine wheels to compare the different modes, such as the velocity and torque parameters of the 18-blade water turbine installation for both wheels. In this study, when considering the torque coefficients, as non-dimensional measurements of the torque produced by a given size of wheel rotor at the water speed, Fig. 10 shows the torque coefficient curves of water turbines in the azimuth angle locations at flow rates of 0.0010–0.0030 m^3/s. The rotation speeds of the water turbine wheels are compared to the torque coefficient values computed using CFD simulations. The torque coefficient has converged and is undergoing large periodic changes, and there are large torque differences near the low and high points of the torque curves. In general, the smaller the time step, the higher the calculation accuracy. This study selects the simulation time step based on calculation time and accuracy.

The empirical simulation results in this study on the proposed vertical-axis small water turbine for installation in the drainage line are summarized in Table 1. The numerical simulation results obtained from the calculations demonstrate the efficiency of a set of water turbine wheels capable of extracting the energy obtained from the water flowing through the drain at different rates. Studies have shown that the torque and mechanical power produced by a water turbine depend on the flow rate, water speed, and rotation speed. The calculated CFD parameters can then be applied to the design of various small turbine wheel sets for further high performance. The CFD simulation results of the study are shown in Fig. 9 and Table 1. The maximum torque and power generated by a small vertical-axis water turbine when installed in drainage lines at a maximum flow rate of 0.0030 m^3/s are 0.55 N.m and 26.84 watts, respectively. Similarly, the maximum mechanical power value after calculating the rate of loss within the pipe system is 12.95 watts when calculated using equations (13). However, overall efficiency can never be 100% since extracting 100% of the kinetic energy of flowing water requires the flow to cease. The conversion efficiency of a hydroelectric power plant is mostly determined by the kind of water turbine used and may be as high as 90-95% for large installations (Woodbank Communications Ltd, 2005; Marco, 2015). As a design guide, the small water turbines in this study achieved 80% performance efficiency.

5.2 Stress Analysis Results

In this paper, the rigidity of PVC material for designing water turbine wheels is determined, and stainless-steel materials are assigned to model the shaft and bearing units. The material properties of stainless steel and PVC rigid were selected with Young's modulus, Poisson's ratio, shear modulus, and mass density. The material properties are shown in Table 2.

The forces caused by water speed can subsequently be applied to the water turbine wheel structure. The vertical-axis small water turbine generator for installation in a pipeline was analyzed under its self-weight by applying a gravitational acceleration of 9.81 m/s^2 in Solidworks Simulation.

A static analysis of the vertical-axis small water turbine for installation in drainage lines is presented in this study using the numerical simulation results calculated and exported to simulation. Static analysis was carried out at 197, 295, 393, 492, and 590 rpm, respectively. Selection constraints were fixed at both ends of the shaft. Subsequently, the properties of the element for analysis can be set to solid mesh, curvature-based mesh, or Jacobian points for a high-quality mesh of 16 points. The mesh element was subdivided into 159,652 by the type of tetrahedron element. The Solidworks simulation results are discussed in the next paragraph.

Table 1
Basic document specifications.

Volume flow rate (m^3/s)	Flow rate (L/min)	Velocity (m/s)	Speed (RPM)	Speed (rad/s)	Torque (N.m) (CFD)	Pressure Drop (m) (CFD)	Power (watt) (CFD)	Power (watt) (Calculation)
0.0010	60	0.494	197	20.58	0.093	0.34	5.91	4.31
0.0015	90	0.740	295	30.84	0.144	0.39	7.44	6.47
0.0020	120	0.987	393	41.13	0.212	0.42	9.72	8.63
0.0025	150	1.234	492	51.42	0.313	0.48	16.09	10.79
0.0030	180	1.481	590	61.71	0.435	0.55	26.84	12.95

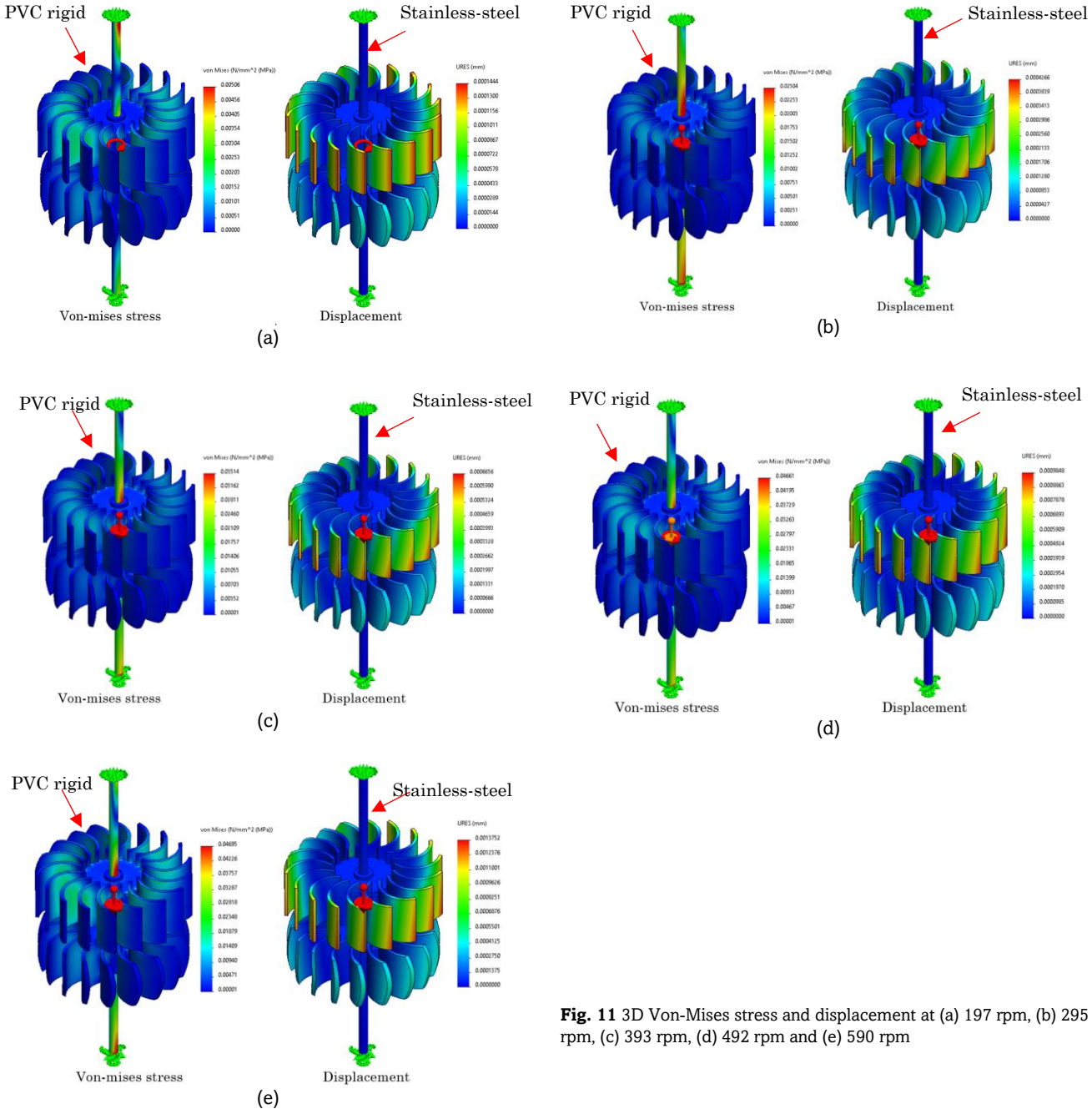

Fig. 11 3D Von-Mises stress and displacement at (a) 197 rpm, (b) 295 rpm, (c) 393 rpm, (d) 492 rpm and (e) 590 rpm

Table 2
Material Parameters (SOLIDWORKS, 2022).

Values	PVC rigid
Young's modulus	2,410 MPa
Poisson's ratio	0.3825
Shear modulus	866.7 MPa
Mass density	1,300 kg/m^3
Values	**Stainless-steel**
Young's modulus	200,000 MPa
Poisson's ratio	0.28
Shear modulus	77,000 MPa
Mass density	7,800 kg/m^3

This section discusses two materials suitable in the manufacture of turbine blades for a water turbine for installation in drainage lines, such as stainless steel and rigid PVC. The materials for the manufacture of turbine blades and tests turbine blade strength are also investigated using FEA. The finite element models for both material types in this study are shown in Fig.11. The maximum von Mises stresses on the water turbine's wheels at 590 rpm are shown in Fig.11(e). When considering the force of the water speed exerted on the turbine wheel structure, the total deformation, showed the highest value at the tip of the blade structure. The maximum value of total deformation at a rotation speed of 590 rpm is 0.001375 mm, as shown in Fig. 11(e). The wheels of a water turbine had a maximum rotation speed of 590 rpm, a safety factor of 15 ul maximum, and a minimum of 2.453. The safety factor values obtained in this research can be used for optimum design.

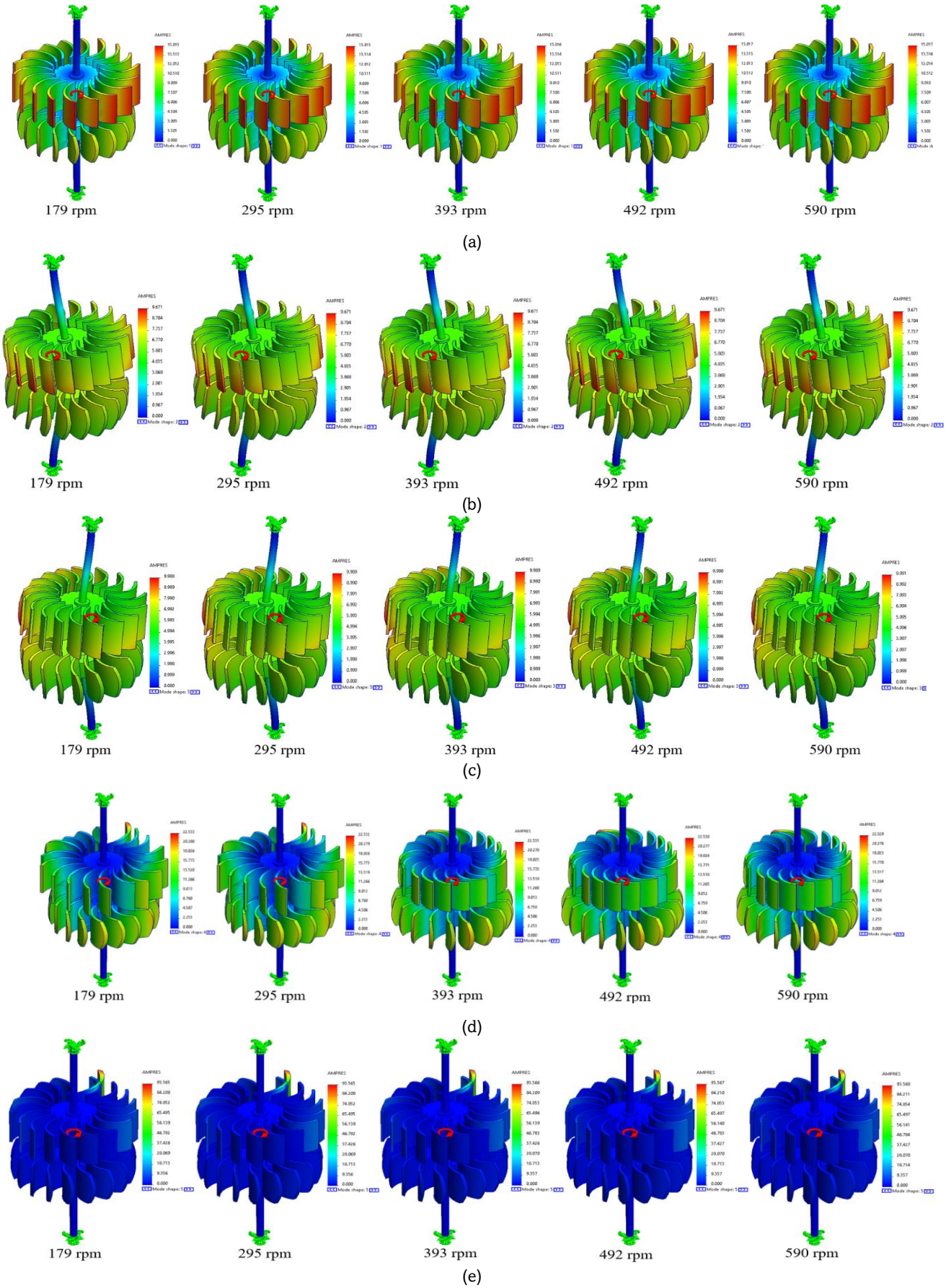

Fig. 12 Maximum natural frequency of mode shape for (a) mode shape 1; (b) mode shape 2; (c) mode shape 3; (d) mode shape 4; (e) mode shape 5

Table 3
The natural frequency values of the vibration shape obtained from analysis.

Mode Shape	Frequency (Hz.)				
	179 (RPM)	295 (RPM)	393 (RPM)	492 (RPM)	590 (RPM)
1	15.015	15.015	15.016	15.017	15.017
2	9.671	9.671	9.671	9.671	9.671
3	9.988	9.989	9.989	9.990	9.991
4	22.533	22.532	22.531	22.536	22.529
5	93.565	93.565	93.566	93.567	93.568

5.4 Frequency analysis results

An analysis of the natural frequencies in this research was conducted and performed on a range of rotational cycles for the water turbine blades. A water turbine wheel rotating at 197, 295, 393, 492, and 590 rpm yielded the results presented in Table 3. The calculation of the natural frequency values obtained from the commercial software and a summary of the analysis results in shape mode are shown in Table 3. The results are also compared at each rotation speed of the turbine blade, as illustrated in Fig. 12.

The geometry of the water wheel set is calculated using mathematical equations and optimized for finite element analysis. The behavioral results obtained by analyzing the natural frequencies generated by vibration at rotational speeds of 179, 295, 393, 492, and 590 rpm for each of the vibration shapes of the water turbine blades are depicted in Fig. 12. According to the finite element models of the frequency mode formed for both material types used in this analysis, the maximum mode shapes of natural frequencies are based on different rotation speed ranges. The results can be summarized as 93.565, 93.566, 93.567, and 93.568, respectively.

Considering the frequency shape at 5, the maximum value obtained from the analysis in Table 3 shows significantly similar values. The natural frequency values affecting vibrations at different rotational speeds are mainly formed in the direction of the Y-axis. After deriving the best model from the CFD analysis, FEA analyses were carried out on the wheels and blades, allowing the stresses and maximum values of the natural frequency to be calculated. The prediction of water turbine performance by FEA analyses, therefore, provides data on the loading of water velocity forces inside the water turbine model. It also gives information on the water force patterns that produce an optimum design for the development of a novel vertical-axis micro water turbine. The vertical-axis small water turbine generator for installation in a drainage line measuring 48 mm diameter was tested in a drainage line with a flow inlet of 50.8 mm or 2 inches. The vertical-axis water turbine (Zhuohuan *et al.,* 2020) was fitted to a set of pipes with a diameter of 100 mm and tested at a speed of 2.1 m/s, with a generating capability of up to 18.3 watts at a rotational speed of 579 RPM. When comparing the numerical simulation results in the field of electricity generation between Zhuohuan *et al.* and the novel vertical-axial small water turbine generator for installation in the drain line, a difference of 31.81% was found.

The numerical results obtained by CFD and FEA simulations lead to the further development of prototypes for small turbines installed in a drainage line to produce electricity. Based on the results of the study and the design of the vertical-axis small water turbine generator for installation in a drainage line in this research, this type of vertical-axis small water turbine can be applied to any closed flow drainage line. The water turbine shape developed is intended to be easily fitted to various types of water drainage lines. Besides, it can be adjusted with nuts and screws to enable disassembly if required

6. Conclusions

This study investigates the optimization of the power output to maintain the performance of vertical axis small water turbines installed into a drainage line system. From the observations made in this research, it can be concluded that the vertical-axis small water turbine generator is suitable for water pipeline and drainage line systems. The mechanical efficiency appears to be 80% for different head and water flow rates. In addition, the actual analysis results are based on theoretical and experimental fluid computation. The basics of designing and analyzing the mechanical parts of the small vertical-axis water turbine generator for installation in pipelines are based on the general principles of water turbine design after determining the available specifications

The completion of FEA numerical simulations can enable the calculation of deformation results and natural frequencies. CFD simulation calculates the results of rotational speeds and the level of power water turbines are ultimately able to produce. The mechanical efficiency, designed and calculated to at around 80%, is very good for a novel vertical axis small water turbine generator designed for installation in a drainage line.

The calculation of variables derived from mathematical equations and numerical simulation appears to be the best combination for constructing an efficient vertical axis micro water turbine generator to be installed in a drainage line. Furthermore, successful implementation will help to alleviate power demands in Thailand with minimal installation costs and negligible maintenance.

Acknowledgments

The authors would like to thank everyone who assisted in this study, including the team at the Division of Energy Technology, School of Energy, Environment, and Materials, King Mongkut's University of Technology Thonburi, who supported the work and helped obtain a high-quality and accurate analysis. Additionally, the authors would like to thank all the friends who gave support and motivation. The first author would also like to thank his family for their spiritual encouragement throughout the process of writing this paper.

Reference

Abdulah, M. and Muhammed, S.D. (2022). Modeling spherical turbine for in-pipe energy conservation. *Ocean Engineering,* 246(2022),110497;https://doi.org/10.1016/j.oceaneng.2021.110497

Anas, A.R., Kumaran, R., Ayu, A.R., Gisrina, E.S. and Lakshuman, D. (2022). Analysis of Wake Turbulence for a Savonius Turbine for Malaysia's Slow-Moving Current Flow. *International Journal of Renewable Energy Development,* 11(4), 1078-1088; https://doi.org/10.14710/ijred.2022.45985

Autodesk Inventor, Autodesk Inventor Professional, Produced by Autodesk Inc., 2015, http:// www.autodesk.com/inventor . Accessed on 18 August 2022.

Autodesk Simulation CFD, Autodesk Simulation CFD, Produced by Autodesk Inc., 2015, http:// www.autodesk.com/cfd . Accessed on 3 November 2022.

Chen, H., Kan, K., Wang, H., Binama, M. and Xu, H. (2021). Development and Numerical Performance Analysis of a Micro Turbine in a Tap-Water Pipeline. *Sustainability,* 13(19), 10755; https://doi.org/10.3390/su131910755

Chen, J., Hongxing, Y., Liu, C.P., Lau, C. H. and Lo, M. (2013). A novel vertical axis water turbine for power generation from water pipelines. *Energy,* 54(2013), 184-193; https://doi.org/10.1016/j.energy.2013.01.064

Culafic, S., Maneski, T. and Bajic, Darko. (2020). Stress Analysis of a Pipeline as a Hydropower Plant Structural Element. *Journal of Mechanical Engineering*, 66(2020), 51-60; https://doi.org/10.5545/sv-jme.2019.6157

ESHA. (2010). *European Small Hydropower Association, Energy Recovery in Existing Infrastructures with Small Hydropower Plants: Multipurpose Schemes Overview and Examples, 2010.* http://www.intechopen.com/download/pdf . Accessed on 6 November 2022.

Ebhota, W.S. and Inambao, F.L (2015). *Domestic Turbine Design, Simulation and Manufacturing for Sub-Saharan Africa Energy Sustainability*. In the 14th International Conference on Sustainable Energy Technologies-SET 2015. https://www.academia.edu/30931929/Domestic_Turbine_Design_Simulation_and_Manufacturing_for_SubSaharan_Africa_Energy_Sustainability

EL-Sayed I.I.M. and Ahmed Farouk A.R., (2019). *In-Pipe Micro-Hydropower Systems for Energy Harvesting*. In 4th IUGRC International Undergraduate Research Conference. https://www.academia.edu/39999108/In_Pipe_Micro_Hydropower_Systems_for_Energy_Harvesting.

Ghada, D., Mohamed, E. and Ahmed, M.A.S. (2022). Performance Assessment of Lift-Based Turbine for Small-Scale Power Generation in Water Pipelines using OpenFOAM. *Engineering Applications of Computational Fluid Mechanics*, 16(1), 536-550; https://doi.org/10.1080/19942060.2021.2019129

Hasanzadeh, N., Payambarpour, S. A., Najafi, A. F., & Magagnato, F. (2021). Investigation of in-pipe drag-based turbine for distributed hydropower harvesting: Modeling and optimization. *Journal of Cleaner Production*, 298, 126710; https://doi.org/10.1016/j.jclepro.2021.126710

Hosain, A., Morteza, K. and Jaber, S. (2020). Experimental investigation and numerical simulation of an inline low-head microhydroturbine for applications in water pipelines. *IET Renewable Power Generation*, 14(16), 3209-3219; https://doi.org/10.1049/iet-rpg.2019.1283

Jiyun, D., Hongxing, Y., Zhicheng, S., & Xiaodong, G. (2018). Development of an inline vertical cross-flow turbine for hydropower harvesting in urban water supply pipes. Renewable *Energy,* 127, 386–397; https://doi.org/10.1016/j.renene.2018.04.070

Jiyun, D., Zhicheng, S. and Hongxing, Y. (2017). Performance enhancement of an inline cross-flow hydro turbine for power supply to water leakage monitoring system. *Energy Procedia*, 145, 363-367; https://doi.org/10.1016/j.egypro.2018.04.065

Ma, T., Yang, H., Guo, X., Lou, C., Shen, Z., Chen, J., & Du, J. (2018). Development of inline hydroelectric generation system_from municipal water pipelines. *Energy*, 144, 535–548; https://doi.org/10.1016/j.energy.2017.11.113

Lahamornchaiyakul, W. (2021). The CFD-Based Simulation of a Horizontal Axis Micro Water Turbine, *Walailak Journal of Science and Technology,* 18(7), 9238; https://doi.org/10.48048/wjst.2021.9238

Muhammad, S.A., Muhammad, A.K., Harun, J., Faisal, J., Alexander, C. and Kim, D.O. (2021). Design and Analysis of In-Pipe Hydro-Turbine for an Optimized Nearly Zero Energy Building. *Sensors,* 21(23), 8154; https://doi.org/10.3390/s21238154

Muhammad, H.T., Shoukat, A.M., Salman, A., Mughees, S., Nouman, Z., Muhammad, A.M., Arsalan, M. and Muhammad, A.S. (2020). Production of electricity employing sewerage lines using a micro cross flow turbine. *International Journal of Engineering, Science and Technology,* 12(2), 67-77; https://doi.org/10.4314/ijest.v12i2.8

Mosbahi, M., Ayadi, A., Mabrouki, I., Driss, Z., Tucciarelli, T., Abid, M.S. (2019). Effect of the Converging Pipe on the Performance of a Lucid Spherical Rotor. *Arab. J. Sci. Eng*, 44, 1583–1600; https://doi.org/10.1007/s13369-018-3625-0

Marco, C. (2015). Harvesting energy from in-pipe hydro systems at urban and building scale. *International Journal of Smart Grid and Clean Energy*, 4(4), 316-327; https://doi.org/10.12720/sgce.4.4.316-327

McLean, D. (Eds.) (2012). *Understanding Aerodynamics*. John Wiley & Sons, Ltd. Chichester, UK.

Nasir, B.A. (2013). Design of High Efficiency Cross-Flow Turbine for Hydro-Power Plant. *International Journal of Engineering and Advanced Technology,* 2(3), 308-311. https://www.ijeat.org/wp-content/uploads/papers/v2i3/C1115022313.pdf.

Oladosu, T.L. and Koya, O.A. (2018). Numerical analysis of lift-based in-pipe turbine for predicting hydropower harnessing potential in selected water distribution networks for waterlines optimization. *Engineering Science and Technology, an International Journal*, 21(4), 672-678; https://doi.org/10.1016/j.jestch.2018.05.016

Olatunji O.A.S., Raphael, A.T. and Yomi, I.T. (2018). Hydrokinetic Energy Opportunity for Rural Electrification in Nigeria. *International Journal of Renewable Energy Development,* 7(2), 183-190; https://doi.org/10.14710/ijred.7.2.183-190

Prasetyo, H., Budiana, E.P., Tjahjana, D.D.D.P. and Hadi, S. (2018). The Simulation Study of Horizontal Axis Water Turbine Using Flow Simulation Solidworks Application. *IOP Conf. Series: Material Science and Engineering, 308, 012022;* https://doi.org/10.1088/1757899X/308/1/012022

Patel, M. and Oza, N. (2016). Design and Analysis of High Efficiency Cross-Flow Turbine for Hydro-Power Plant. *International Journal of Engineering and Advanced Technology*, 5(4), 187-193.

Posew, K. and Ananchaipattana, C. (2016). Pelton Turbine Efficiency Analysis Using Computational Fluid Dynamics Technique. *Journal of Engineering*, RMUTT 14(2), 11-18. https://ph01.tci-thaijo.org/index.php/jermutt/article/view/242005.

Samora, I., Hasmatuchi, V., Münch-Alligné, C., Franca, M.J., Schleiss, A. J., & Ramos, H. M. (2016). Experimental characterization of a five-blade tubular propeller turbine for pipe inline installation. *Renewable Energy*, 95, 356–366. https://doi.org/10.1016/j.renene.2016.04.023

Sritram, P., Wichian, P., Suwansri, S. and Suntivarakorn R. (2017). The Effects of Turbine Buffle Plates on the Efficiency of Water Free Vertex Hydro Turbine. *Frame Engineering and Automation Technology Journal*, 3 (1), 45-52. https://ph02.tci-thaijo.org/index.php/featkku/article/view/176547/125918.

Sinagra, M., Sammartano, V., Aricò, C., Collura, A. and Tucciarelli, T. (2014). Cross-flow turbine design for variable operating conditions, *Procedia Engineering,* 70, 1539–1548. https://org/10.1016/j.proeng.2014.02.170

Solidworks, Solidworks Simulation, Produced by Solidworks Corporation., 2022, https://www.solidworks.com/. Accessed on 12 October 2022.

Sukha, W., Kaewrueng, S., Thuwapanichayanan, R., Sermsak, R. (2019). Assessment of Rainfall Through Reflectivity and Rainfall Intensity Relationship at Phitsanulok Weather Radar Station. *Journal of Kanchanaburi Rajabhat University*, 9(1), 137-149. https://so03.tci-thaijo.org/index.php/KRUjournal/article/view/206127.

Sobachkin, A. and Dumnov, G. Numerical Basis of CAD-Embedded CFD. NAFEMS World Congress., 2013, https://www.solidworks.com/ . Accessed on 3 November 2022.

Thomas, J.V. and Thomas, G. (2019). Micro turbines at Drinking Water Tanks Fed by Gravity Pipelines: A Method and Excel Tool for Maximizing Annual Energy Generation Based on Historical Tank Outflow Data. *Water*, 11(7), 1403; https://doi.org/10.3390/w11071403

Tiaple Y., sritrakul N., Nontakaew U. and chamamahattana P., 2008. Blade Shape Design for Small Axial Flow Hydro Turbine. In The

22ed conference of mechanical engineering network of Thailand (ME-NETT22). Pathumthani, Thailand, 15-17 October. Mechanical Engineering, Thammasat University Publishers.

Uchiyama, T., Honda, S., Okayama, T. and Degawa T. (2016). A Feasibility Study of Power Generation from Sewage Using a Hollowed Pico-Hydraulic Turbine. *Engineering* 2(4), 510-517; https://doi.org/10.1016/J.ENG.2016.04.007

Vaishaly, P. and Romarao, S. (2015). Finite element stress analysis of a typical stream turbine blade. *International Journal of Science and Research* (IJSR), 4(7), 1059-1065. https://www.ijsr.net/archive/v4i7/SUB156518.pdf.

Wisatesajja, W., Roynarin, W., Intholo, D. (2021). Analysis of Influence of Tilt Angle on Variable-Speed Fixed-Pitch Floating Offshore Wind Turbines of Optimizing Power Coefficient Using Experimental and CFD Models. *International Journal of Renewable Energy Development*, 10(2), 201-212; https://doi.org/10.14710/ijred.2021.33195

Woodbank Communications Ltd, (2005). Hydroelectric Power. Retrieved 12 October 2022, from https://www.mpoweruk.com/hydro_power.htm .

Yeo, H., Seok, W., Shin, S., Huh, Y.C., Jung, B.C., Myung, C.S. and Rhee, S.H. (2019). Computational Analysis of the Performance of a Vertical Axis Turbine in a Water Pipe. *Energies*, 12(20), 3998; https://doi.org/10.3390/en12203998

Zhuohuan, H.U., Dongcheng, W., Wei, L.U., Jian, C. and Yuwen, Z. (2020). Performance of vertical axis water turbine with eye-shaped baffle for pico hydropower. *Front. Energy*, 1-4; https://doi.org/10.1007/s11708-020-0689-9